



Cite this: *Chem. Commun.*, 2018, 54, 9259

Two-dimensional self-assembled nanostructures of nucleobases and their related derivatives on Au(111)

Yuanqi Ding, Xinyi Wang, Lei Xie, Xinyi Yao and Wei Xu *

The construction of two-dimensional (2D) self-assembled nanostructures has been one of the considerably interesting areas of on-surface chemistry in the past few decades, and has benefited from the rapid development and improvement of scanning probe microscopy techniques. In this research field, many attempts have been made in the controllable fabrication of well-ordered and multifunctional surface nanostructures, which attracted interest because of the prospect for artificial design of functional molecular nanodevices. DNA and RNA are considered to be programmable self-assembly systems and it is possible to use their base sequences to encode instructions for assembly in a predetermined fashion at the nanometer scale. As important constituents of nucleic acids, nucleobases, with intrinsic functional groups for hydrogen bonding, coordination bonding, and electrostatic interactions, can be employed as a potential system for the versatile construction of various biomolecular nanostructures, which may be used to structure the self-assembly of DNA-based artificial molecular constructions and play an important role in novel biosensors based on surface functionalization. In this article, we will review the recent progress of on-surface self-assembly of nucleobases and their derivatives together with different reactants (e.g., metals, halogens, salts and water), and as a result, various 2D surface nanostructures are summarized.

Received 4th May 2018,
Accepted 10th July 2018

DOI: 10.1039/c8cc03585g

rsc.li/chemcomm

Interdisciplinary Materials Research Center, Tongji-Aarhus Joint Research Center for Nanostructures and Functional Nanomaterials, College of Materials Science and Engineering, Tongji University, Shanghai 201804, P. R. China.
E-mail: xuwei@tongji.edu.cn



Wei Xu

Prof. Wei Xu received his PhD degree in Science from Aarhus University, Denmark, in 2008. Thereafter he was a postdoctoral fellow at the Interdisciplinary Nanoscience Center (iNANO), Aarhus University, Denmark, and at the Departments of Chemistry and Physics, The Penn State University, USA. Since 2009 he has been a full professor at Tongji University, P. R. China. His main research interests are Scanning Tunneling Microscopy (STM) and

Density Functional Theory (DFT) investigations of molecular self-assemblies and reactions on surfaces under ultrahigh vacuum conditions with the aim of controllably building functional surface nanostructures and gaining fundamental insights into physics and chemistry.

Introduction

Surface-based supramolecular chemistry, which relies on non-covalent interactions, has been widely employed as an appealing and efficient way for controllable fabrication of highly complex and multifunctional surface nanostructures through self-assembly processes from rationally designed and selected molecular building blocks.^{1–11} With the development of scanning probe microscopy (SPM) techniques in the past few decades, atomically precise fabrication of a variety of supramolecular nanostructures to generate multiple dimensions and patterns on surfaces has become an innovative and challenging strategy towards artificial design of functional molecular nanostructures and nanodevices.^{12–17} To get more and more complicated nanostructures, many attempts have been made, for example, by designing molecular precursors with various functional groups embedded, introducing different kinds of metals, and selecting different substrates with requisite chemical properties and lattices.^{4,10,11,18–36}

It has been reported that biomolecules like deoxyribonucleic acid (DNA) and ribonucleic acid (RNA) are marvelous building blocks suitable for the design and formation of sophisticated nanostructures by self-assembly since the system is rich in hydrogen bonds and it is possible to use the complementary base sequences for assembly in a predetermined fashion at the

nanometer scale.^{37–42} As the key constituents of nucleic acids, nucleobases (guanine (G), cytosine (C), adenine (A), thymine (T) and uracil (U)) with intrinsic and abundant hydrogen bonding sites are considered to be a potential system for the construction of various on-surface supramolecular nanostructures. Those nanostructures based on biomolecules *via* hydrogen bonding play an important role in the novel biosensors based on surface functionalization and can also be used to structure the self-assembly of DNA-based artificial molecular constructions. In the meantime, the introduction of other reactants (such as metals, halogens, salts and water) has been proven to be an efficient approach to tune the self-assembled structures. As a result, various nanostructures which are stabilized by hydrogen bonds, coordination bonds, and electrostatic interactions are fabricated. Besides, some of the reactants (*e.g.*, water, metals) have been found to be able to influence the tautomerization of nucleobases,^{36,43–66} which could further influence the formed nanostructures. Therefore, the atomic-scale investigations on the fundamental interactions between nucleobases and the above mentioned reactants would be of general interest for both physical chemistry and biochemistry to understand the underlying mechanism.

In this article, we will summarize a series of 2D nanostructures constructed by nucleobases (including their derivatives) interacting with various reactants mentioned above on surfaces, as well as the self-assembled structures of nucleobases themselves like base pairings. The nucleobase derivatives are modified at the same sites as those of the natural nucleosides (*i.e.*, N9 site for purine and N1 site for pyrimidine) which are used to connect with ribose groups in the natural nucleosides. The Au(111) surface is employed as a template to ensure that the molecules adopt flat adsorption geometries to facilitate the formation of 2D nanostructures.^{67–72} Most experiments are performed using scanning tunneling microscopy (STM) under ultra-high vacuum (UHV) environments with the aim of gaining sub-molecularly resolved STM images of self-assembled structures, and from the combination of density functional theory (DFT) calculations the underlying fundamental mechanisms are explored. It is noted that there are plenty of excellent works related to nucleobase molecules by means of spectroscopic methods, and biological experiments have contributed in this field. In this article we mainly focus on STM-based structure investigations and do not discuss the other related spectroscopic works. In the following sections, we will show 2D nanostructures constructed by nucleobases (including their derivatives) and (i) metals; (ii) halogens; (iii) salts; (iv) water; and (v) nucleobases themselves.

2D nanostructures constructed by nucleobases and metals

Metal–organic bonding originated from organometallic and coordination chemistry has been extensively employed by the surface science community to grow highly ordered supramolecular surface nanostructures, in which alkali metals (such as K, Na) and transition metals (such as Fe, Ni) are involved as the main

metal sources.^{18,19,29–31,33} In general, nucleobases can afford multiple N and/or O binding sites to interact with metal atoms, resulting in various motifs *via* coordination or electrostatic interactions, which further form the 2D nanostructures normally by intermolecular hydrogen bonds.

Alkali metals

Alkali metals are known to play a vital role in several cellular environments. For example, as important cations *in vivo*, potassium ions (K^+) can stabilize the G-quadruplex structure and inhibit the activity of telomerase.⁷³ Xu *et al.*^{74,75} reported that mobile G molecules on the Au(111) surface can interact with K atoms by electrostatic interactions, resulting in the formation of two different metallosupramolecular networks that are both stabilized by a delicate balance between intermolecular hydrogen bonding and electrostatic interactions. Fig. 1 shows the STM images and the DFT relaxed model of the G-quartet-K network at a relatively low K dose.⁷⁴ The K atom can be resolved as a protrusion in the center of the G-quartet (*i.e.*, the G_4K_1 motif), which is further linked together by intermolecular hydrogen bonds leading to the G_4K_1 metallosupramolecular network on Au(111). At a relatively high K dose, the metallosupramolecular structure can be tuned to a porous network,⁷⁵ whose elementary building block is composed of three G molecules and two K atoms (*i.e.*, the G_3K_2 motif). The stabilization of various G-K networks on the surface results from the cooperative effect of hydrogen bonds and electrostatic interactions, which shows the significance of alkali metals in the nucleobase related 2D self-assembled structures.

Transition metals

Owing to the advantages of diversity and constitutional dynamic characteristics of coordination bonds, transition metals have been widely used in constructing flexible nanostructures on surfaces, while this kind of supramolecular nanostructure with constitutional diversity and adaptability would be of fundamental importance for potential application in molecular switching devices. The fundamental interactions between G and Ni were investigated by Kong *et al.* in 2014.⁷⁶

Sequential co-deposition of G molecules and Ni atoms followed by annealing at 420 K leads to the formation of a kind

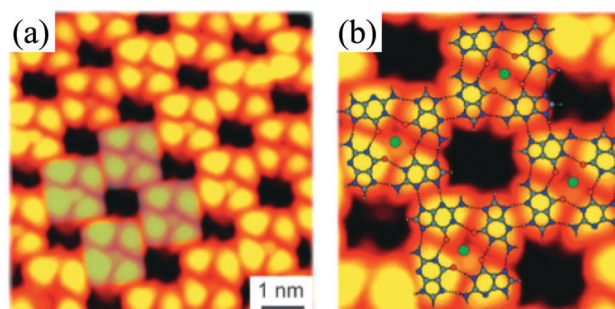


Fig. 1 STM images and DFT optimized structural model of the G-quartet-K network on Au(111). (a) The high-resolution STM image of the G_4K_1 network. (b) The DFT relaxed model superimposed on the close-up STM image.⁷⁴ Reproduced with permission from Royal Society of Chemistry.

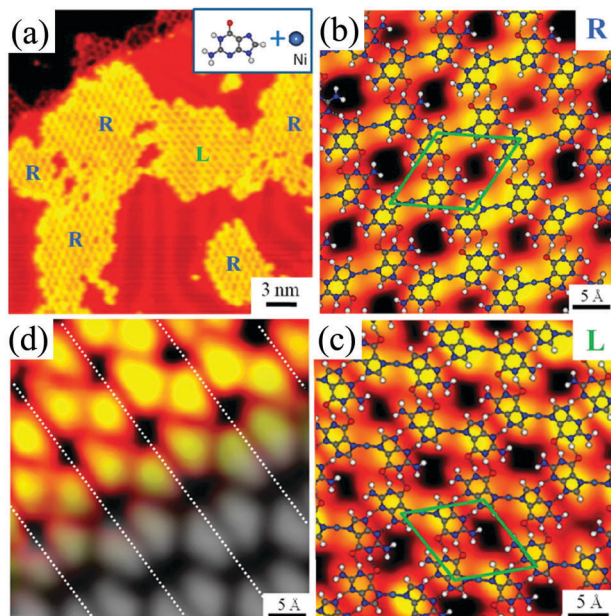


Fig. 2 STM images, DFT-based optimized structural models and simulated STM image of the G and Ni-coordinated metallosupramolecular network on Au(111). (a) The STM image shows the self-assembled nanostructures with each island being homochiral (as indicated by R and L) formed by G and Ni. (b and c) DFT-optimized structural models superimposed on the corresponding close-up STM images. The green parallelogram represents the unit cell of the nanostructure. (d) The simulated STM image (the gray part) is partially superimposed on the STM image.⁷⁶ Reproduced with permission from American Chemical Society.

of metallosupramolecular network with different chiralities as shown in Fig. 2. High-resolution close-up STM images (Fig. 2b and c) depict the enantiomerically pure R and L chiral structures, respectively, with the DFT-optimized structural models superimposed. From the models, it can be identified that all the G molecules are coordinated with the Ni atom at the

N7 site. Interestingly, the N7 site happens to be the site for proton transfer from N9 when tautomerization from G/9H to G/7H occurs. Therefore, G molecules and Ni atoms form 2D networks on Au(111) with the assistance of coordination bonds and hydrogen bonds, which further effectively inhibit the tautomerization from G/9H to G/7H by screening the corresponding proton transfer site.

Another nucleobase molecule, thymine (T), contains two possible coordination binding sites, both of which are capable of coordinating to Ni atoms with similar stability as revealed by theoretical calculations. Thus, Kong *et al.*⁷⁷ chose T and Ni atoms as a potential model system to present structural diversity, which further allowed the investigation of dynamic coordination chemistry on the surface. In this system, the metallosupramolecular structures formed by T and Ni are constructed on Au(111), and moreover continuous interconversions between 1D metal-organic chains and 2D hybrid honeycomb networks (Fig. 3) are achieved on the surface. From the close-up STM image of the 2D honeycomb network structure (Fig. 3a), it can be identified that the structure is composed of both trimeric and dimeric elementary motifs as indicated by green and blue contours, respectively (Fig. 3b). The DFT optimized model shows that the trimer is formed by three T molecules coordinating to one Ni atom, and the dimeric motif is assigned to a hydrogen-bonded T dimer (as shown in detail in Fig. 3c).

It has been reported previously by Wang *et al.*⁷⁸ that co-deposition of 9-ethylguanine (9eG, a modified guanine) molecules and Fe atoms at a certain ratio on Au(111) at room temperature (RT) resulted in the formation of well-ordered G-quartet-Fe complex arrays. On this basis, Zhang *et al.*^{79,80} took the advantage of dynamic characteristics of coordination bonds to construct a series of 2D nanostructures on the surface and realized the continuous and reversible structural transformations at RT. Fig. 4a–h show an overview of the gradual structural transformations of various surface nanostructures,

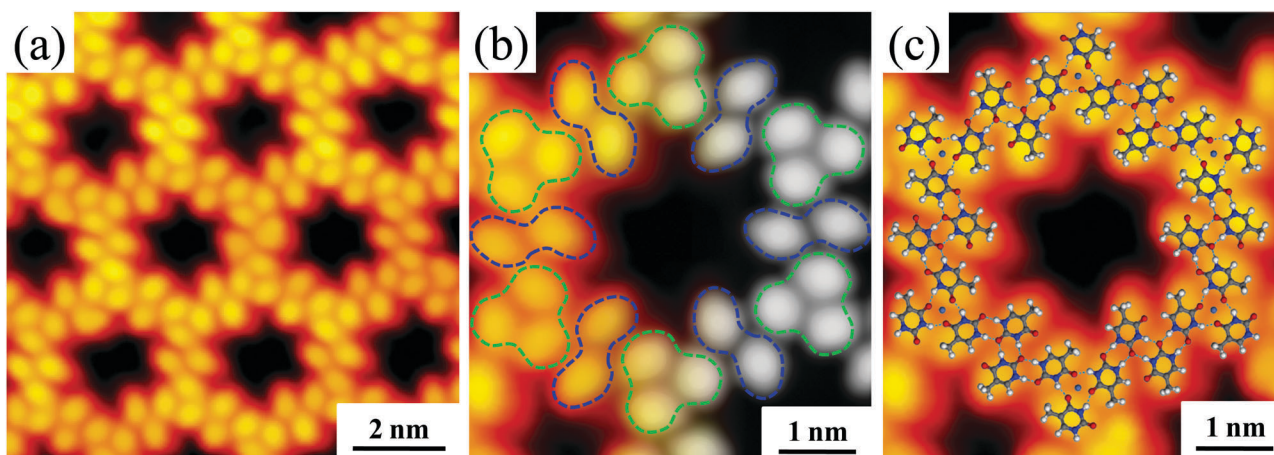


Fig. 3 STM images, simulated STM image and DFT-based optimized structural models of a hybrid molecular network composed of metal-organic T_3Ni_1 trimers and hydrogen-bonded T dimers on Au(111). (a and b) Close-up high-resolution STM images of hybrid molecular networks allowing us to identify the individual building blocks (*i.e.*, metal-organic T_3Ni_1 trimers and hydrogen-bonded T dimers indicated by green and blue contours, respectively) within the network structure. The STM simulation (the gray part) is partially superimposed on the STM image. (c) DFT-optimized structural model superimposed on the STM image.⁷⁷ Reproduced with permission from John Wiley and Sons.

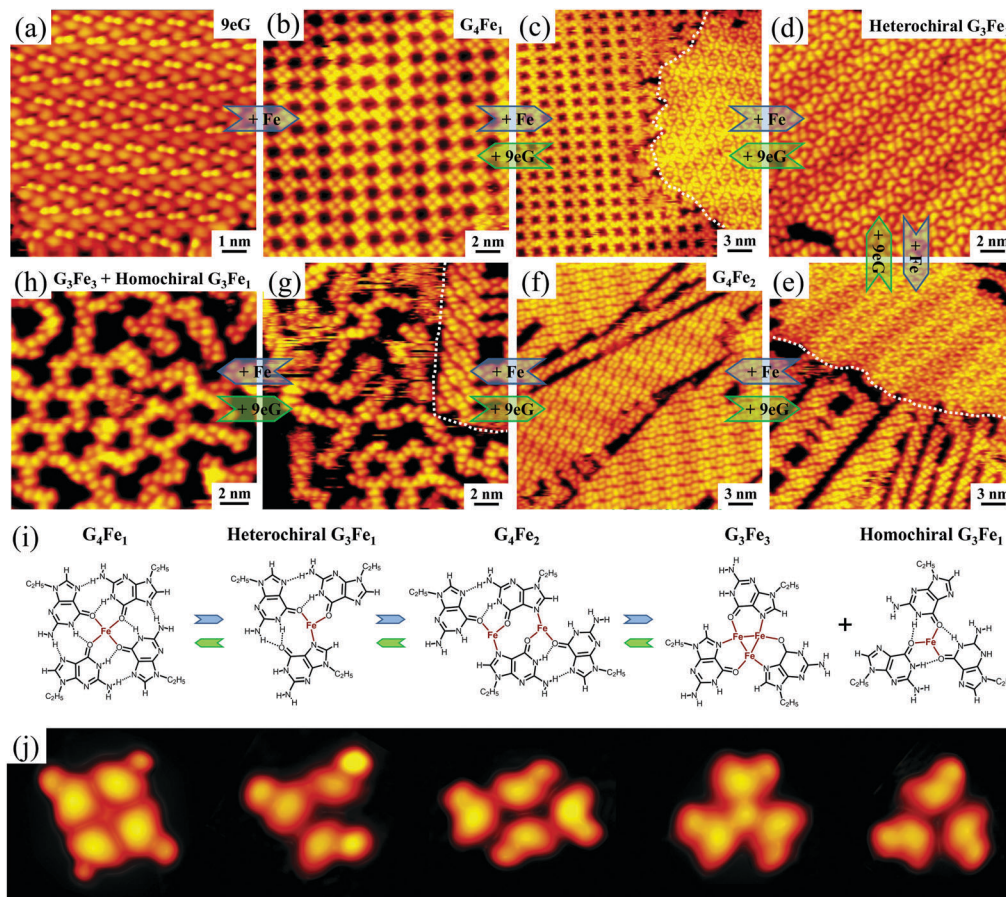


Fig. 4 (a–h) STM images showing the structural transformations in response to Fe atoms. (a) Formation of the 9eG island at RT. Structural transformations among (b) G_4Fe_1 , (d) heterochiral G_3Fe_1 , (f) G_4Fe_2 , and (h) G_3Fe_3 together with homochiral G_3Fe_1 motifs on the Au(111) surface after stepwise dosing of Fe atoms on the sample obtained in the last step at RT. (c, e and g) STM images showing coexistence of the two respective structures within the transformations. (i and j) The structural models and the corresponding close-up STM images of these metal–organic motifs.⁷⁹ Reproduced with permission from John Wiley and Sons.

namely, 9eG island (Fig. 4a), G_4Fe_1 network (Fig. 4b), heterochiral G_3Fe_1 island (Fig. 4d), G_4Fe_2 island (Fig. 4f), and hexagonal ring networks (Fig. 4f) composed of G_3Fe_3 together with homochiral G_3Fe_1 motifs, in response to delicately controlled Fe dosages at RT. Note that such structural transformations can be reversed through controlled depositions of 9eG on a certain structure-covered surface at RT. The structural models and the corresponding high-resolution STM images of the involved metal–organic elementary motifs are shown in Fig. 4i and j, respectively. The study systematically shows the on-surface reversible structural transformations of multiple metal–organic motifs with different binding modes in response to both Fe and 9eG, where the intrinsic dynamic characteristic of coordination bonds and the coordination priority and diversity are found to be the key.

Apart from the structural transformation in response to the constituents, different metal–organic nanostructures in response to the substrate temperatures have also been demonstrated in the system of 9eG molecules and Ni atoms.⁸¹ Co-deposition of 9eG and Ni with different stoichiometric ratios followed by further annealing at 390 K on the Au(111)

surface results in the formation of two typical nanostructures (rhomboid network and 1D chain) composed of G_3Ni_1 (Fig. 5a–c) and G_2Ni_2 motifs, respectively, and also the reversible transformations between these two structures are achieved in response to both 9eG molecules and Ni atoms owing to the dynamic characteristics of coordination bonds. A close-up STM image of the rhomboid network (Fig. 5b) allows us to identify the individual molecular chiralities (as indicated by L and R notations). The elementary G_3Ni_1 motifs with different chiralities are depicted by green and blue contours, respectively, and a 9eG dimer is depicted by a white contour. The close-up STM image of the G_3Ni_1 motif superimposed with the DFT-optimized model is shown in Fig. 5c. Furthermore, by delicately controlling the substrate temperature, *i.e.*, after codeposition of 9eG and Ni simultaneously on Au(111) held at a high temperature of 430 K, a honeycomb network composed of G_3Ni_3 motifs (Fig. 5d) has been formed. The elementary G_3Ni_3 motifs are depicted by white contours (Fig. 5e). The close-up STM image of the G_3Ni_3 motif superimposed with the DFT-optimized model is shown in Fig. 5f.

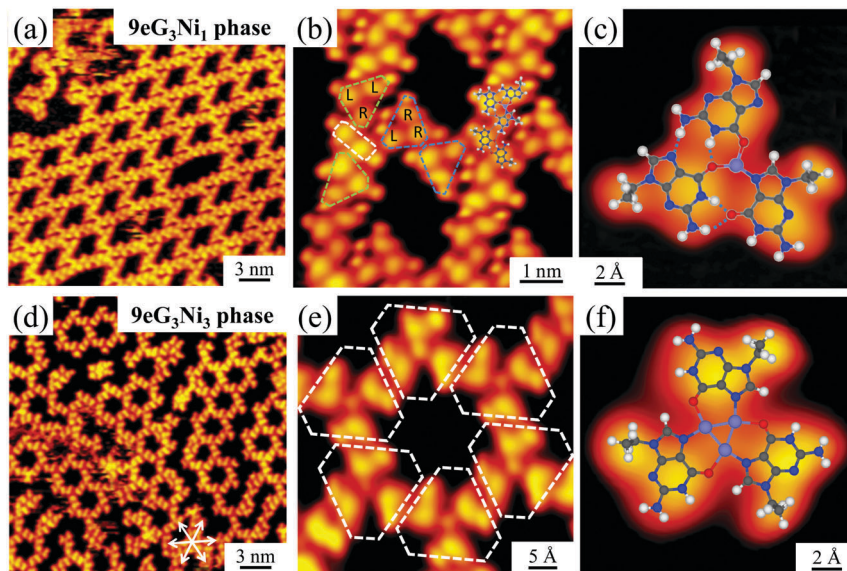


Fig. 5 STM images and DFT models of (a–c) the rhomboid network composed of metal–organic G_3Ni_1 motifs and hydrogen-bonded G dimers after deposition of 9eG molecules and Ni atoms followed by further annealing at 390 K on Au(111). (d–f) The honeycomb network composed of G_3Ni_3 motifs after codeposition of 9eG and Ni simultaneously on Au(111) held at a high temperature of 430 K.⁸¹ Reproduced with permission from John Wiley and Sons.

2D nanostructures constructed by nucleobases and halogens

It is well-known that halogen doping is a widely utilized method in polymer chemistry to transform polyacetylene and polyaniline to conductive polymers.^{82,83} For on-surface chemistry, halogen atoms usually act as byproducts of on-surface dehalogenative reactions^{84–89} or can be trapped as guests in the self-assembled structures,⁹⁰ and moreover, it was shown that the direct introduction of iodine onto metal surfaces under UHV conditions can decouple covalently bonded molecular networks from the surface.⁹¹ Recently, Xie *et al.*⁸¹ introduced iodine (I_2) vapour into the 9eG–Ni and 9eG–Fe systems and demonstrated that the halogens could induce structural transformation and stabilization of metal–organic motifs. Introduction of I_2 vapour to either the G_3Ni_1 or G_2Ni_2 phase and further annealing at 490 K leads to the formation of a honeycomb network structure composed of $G_3Ni_3I_3$ motifs, in which the iodine atoms are homogeneously located at specific hydrogen-rich harbours enclosed by 9eG molecules *via* electrostatic interactions as shown in Fig. 6a and b (the elementary $G_3Ni_3I_3$ motifs and iodine atoms are depicted by white contours and blue circles, respectively). The DFT relaxed structural model is shown in Fig. 6c. In addition, a control experiment demonstrated that the introduction of I_2 vapour to the G_3Ni_3 structure (only formed under harsh conditions) also resulted in the formation of the $G_3Ni_3I_3$ structure, and the existence of iodine atoms was found to be able to further stabilize the G_3Ni_3 structure. As mentioned before,^{79,80} the 9eG molecules and Fe atoms can form various metal–organic structures, while the formation of a pure G_3Fe_3 network is rather difficult. Interestingly, introduction of iodine to this system (at a 9eG/Fe ratio of *ca.* 1 : 1) followed by annealing at 390 K also results in

the formation of a similar honeycomb network composed of $G_3Fe_3I_3$ motifs as shown in Fig. 6d and e. These experiments demonstrate the generality of the unexpected effect of iodine atoms on regulating the formation of specific three-metal centre coordination motifs on surfaces.

2D nanostructures constructed by nucleobases and salts

As can be seen from the above, metal atoms/ions have been extensively employed in the formation and regulation of metal–organic structures, and moreover, halogens are also found to be able to influence the formed structures by electrostatic interactions. Normally, the metals are directly provided from metal sources. However, it would be interesting to note that the direct sublimation of salts can also serve as a versatile way (by simultaneously providing both metals and halogens) to construct surface nanostructures.

For example, the salts, NaCl and LiCl, grown on substrates can be employed as a sort of reactant to effectively interact with the organic molecules to form ionic self-assembled structures.^{92–95} Inspired by this, Zhang *et al.*⁹⁶ directly introduced alkali and alkaline earth salts (NaCl, KBr and $CaCl_2$) to interact with the 9eG molecules on Au(111), in which various G-quartet–M networks (where M denotes Na, K, and Ca, respectively) were formed. Besides, with the aid of NaCl, the tautomeric recognition, separation, and interconversion of G molecular networks (formed by two tautomeric forms G/9H and G/7H) on the Au(111) surface have been achieved.⁹⁷ In this process, the disordered phase of G (normally mixed by G/9H and G/7H) can be converted to G-quartet–Na networks and G/7H islands when interacting with NaCl (Fig. 7a–c), which indicates that the

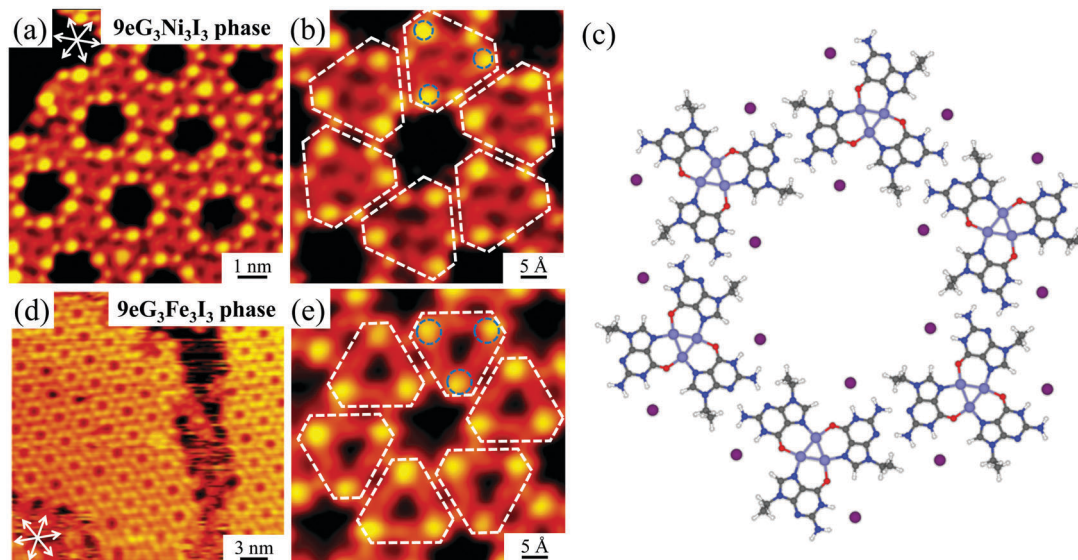


Fig. 6 STM images of the $G_3M_3I_3$ ($M = Ni, Fe$) networks on Au(111) and the DFT-optimized gas-phase model. The elementary $G_3M_3I_3$ motifs are depicted by white contours and iodine atoms are indicated by blue circles. H: white, C: gray, N: blue, O: red, Ni: light blue, I: purple.⁸⁴ Reproduced with permission from John Wiley and Sons.

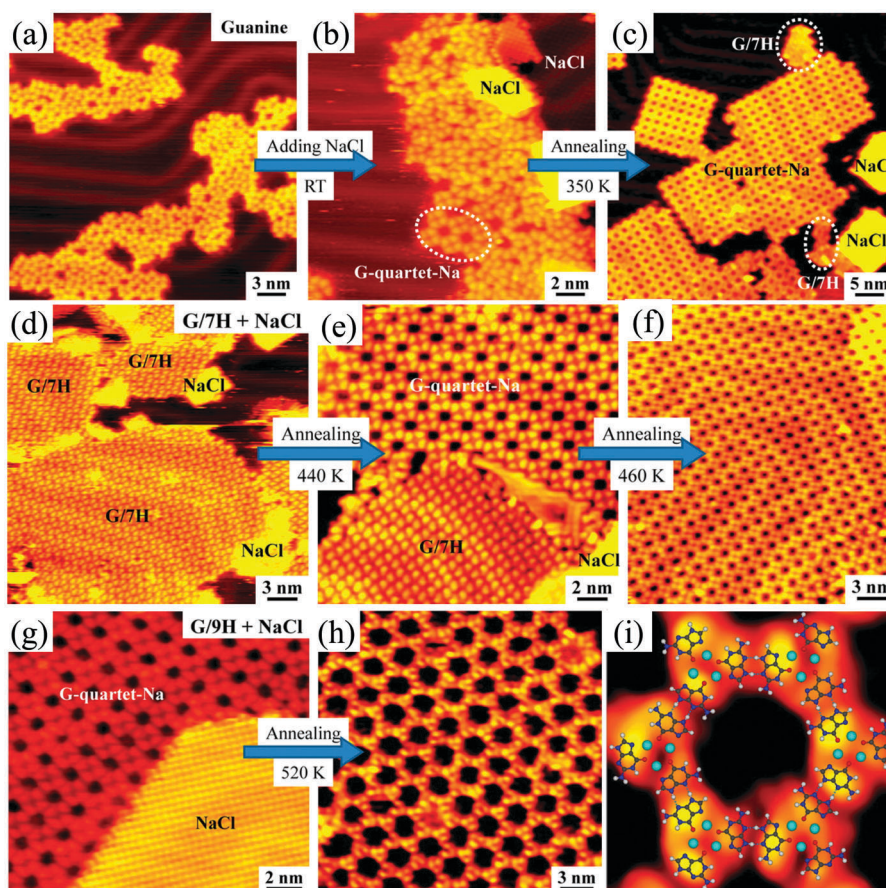


Fig. 7 (a–c) STM images showing the conversion from the disordered structures formed by the mixture of two G tautomers (G/9H and G/7H) to the G-quartet-Na structure (by G/9H) and the G/7H islands with the aid of NaCl on Au(111). (d–f) STM images showing the conversion from the G/7H islands to the G-quartet-Na structure on Au(111). (g and h) STM images showing the transformation from the G-quartet-Na structure to a more open porous structure on Au(111) when further interacting with NaCl. (i) High-resolution STM image of the porous structure with the DFT optimized gas-phase model superimposed.⁹⁷ Reproduced with permission from American Chemical Society.

mixture of two tautomeric forms G/9H and G/7H is separated. Moreover, the G/7H islands can also be converted back to G-quartet-Na networks (Fig. 7d–f), indicating that the tautomerization from G/9H to G/7H is reversible. A step further, dosing more NaCl on G-quartet-Na networks and further annealing at ~ 520 K results in structural transformation from the G-quartet-Na structure to a more open G_3Na_3 network as shown in Fig. 7g–i. As the building block of the new porous structure, the G_3Na_3 motif is similar to the reported structures based on three-metal centers.^{66,98}

To demonstrate the generality, Xie *et al.*⁸¹ chose other salts like $NiCl_2$ and $FeBr_2$ simultaneously providing both metals and halogens to interact with 9eG molecules, in which similar honeycomb network structures as shown in Fig. 6 were achieved and assigned to $G_3Ni_3Cl_3$ and $G_3Fe_3Br_3$, respectively. Moreover, Xie *et al.*⁹⁹ chose another base molecule, *i.e.*, 1-methylcytosine (1mC) molecule, to interact with NaCl to explore the role of halogens in the formation of surface nanostructures. Deposition of NaCl onto the 1mC precovered Au(111) surface and annealing at 370 K leads to the formation of various ordered networks composed of elementary metal-organic C_4Na_2 motifs linked by Cl atoms as shown in Fig. 8. As can be seen from the structural model of C_4Na_2 in Fig. 8a, only hydrogen atoms are available in the periphery of the C_4Na_2 motif, which cannot be connected by themselves through hydrogen bonds, while the halogens just prefer to locate at the hydrogen-rich positions *via* electrostatic interactions to link the C_4Na_2 motifs. Normally, one Cl atom is needed between two adjacent motifs within a single chain (schematics as shown in Fig. 8a). When two chains are laterally linked together in different manners to form networks, more Cl atoms are employed

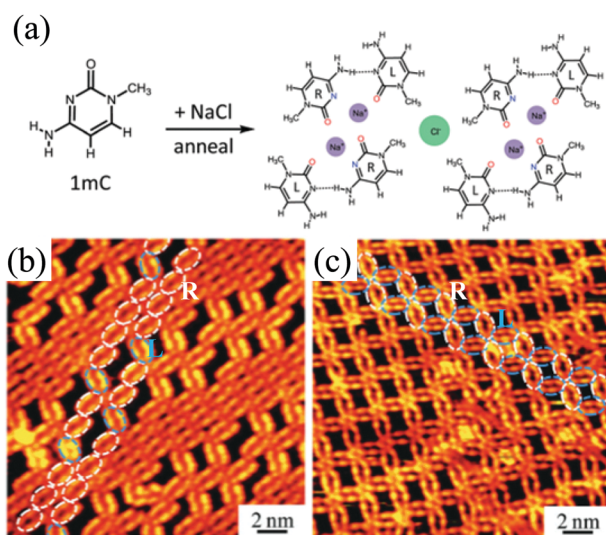


Fig. 8 (a) Schematic illustration of the structural formation of metal-organic motifs mediated by Cl atoms. (b and c) Various ordered networks composed of the metal-organic C_4Na_2 motifs linked by Cl in different manners (linear or zigzag). C_4Na_2 motifs are highlighted by white and blue ellipses showing different chiralities (as indicated by the R and L notations).⁹⁹ Reproduced with permission from Royal Society of Chemistry.

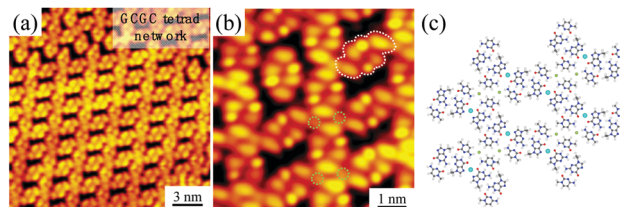


Fig. 9 STM images and DFT optimized gas-phase model of the network structure composed of GCGC tetrads stabilized by both Na and Cl on Au(111). GCGC tetrad motifs and Cl are depicted by white and green contours, respectively. H: white; C: gray; N: blue; O: red; Na: blue; Cl: green.¹⁰⁰ Reproduced with permission from Royal Society of Chemistry.

to form additional weak hydrogen bonds to stabilize the whole structure. Owing to the flexibility and relatively weak electrostatic interactions, the elementary C_4Na_2 motif can be linked together into various network structures as shown in Fig. 8b and c.

Besides, Ding *et al.*¹⁰⁰ also introduced NaCl to a self-assembled GCGC tetrad (formed by two Watson–Crick GC pairs) structure to detect the stability of GCGC tetrads in comparison with the above mentioned G-quartet-Na structure. The codeposition of 9eG and 1mC molecules (at a ratio of 1 : 1) on Au(111) followed by annealing results in the formation of GCGC tetrads which are further connected to a chain structure by hydrogen bonds. After subsequent deposition of NaCl on the GCGC tetrad chains precovered surface and further annealing at 370 K, interestingly, the GCGC tetrad chains transform into a network structure as shown in Fig. 9a. From the high-resolution STM image (Fig. 9b) and the DFT optimized model (Fig. 9c), it is identified that the GCGC tetrads are linked together by both Na (not visible in this case) and Cl without perturbing the intra-tetrad hydrogen bonds, which demonstrates the robustness of such a GCGC tetrad structure.

2D nanostructures constructed by nucleobases and water

The interactions between water and organic molecules on surfaces have been explored by STM with real-space evidence, in which water is found to play a vital role in determining the molecular conformation of a single molecule¹⁰¹ and influencing supramolecular networks of azobenzene molecules.¹⁰² On the other hand, water has been found to play a unique role in relation to the structures, functions, and activities of DNA/RNA molecules *in vivo*, and might also be responsible for the presence of some rare tautomeric forms of nucleobases predicted in theoretical calculations.^{45,46,53} Inspired from those, Zhang *et al.*¹⁰³ introduced water molecules into UHV environments to explore the interactions between nucleobases and water, and as a result, the real-space experimental evidence of a rare G tautomer induced by water has been obtained. Exposure of the G-precovered Au(111) surface to the water atmosphere at a pressure of $\sim 10^{-5}$ mbar and subsequent annealing at 310 K results in the formation of island structures composed of

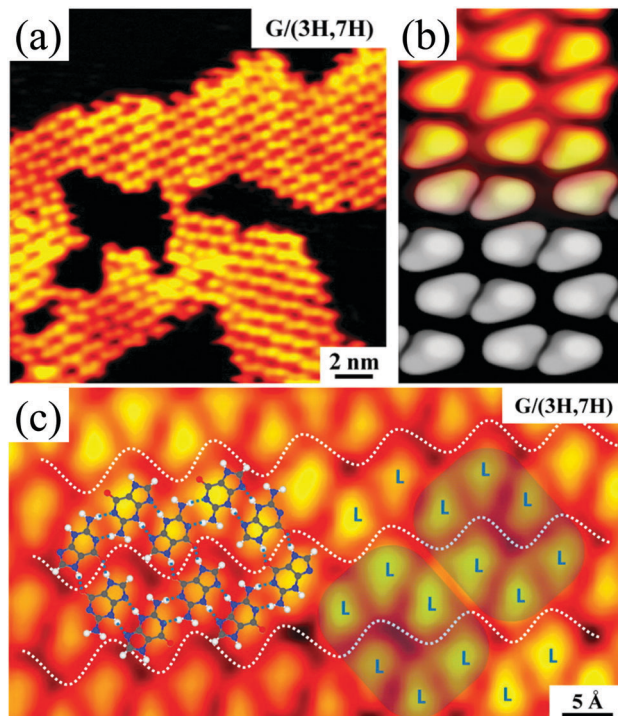


Fig. 10 (a) A large-scale STM image showing the formation of islands composed of a parallel six-membered ring network structure. (b) A close-up STM image partially superimposed with the STM simulation (the gray part). (c) Submolecularly resolved STM image superimposed with the DFT-optimized structural model allowing identification of the molecular chirality (as indicated by L notation).¹⁰³ Reproduced with permission from American Chemical Society.

parallel six-membered ring network structures, as shown in Fig. 10a. From the submolecularly resolved STM image (Fig. 10c), we distinguish that the island is made up of homochiral G molecules, and the whole network structure is enantiomerically pure.

Note that this parallel six-membered ring network is only obtained after exposing the system to a water atmosphere, and neither G/9H nor G/7H form (the two most stable tautomeric forms of the G molecule in the gas phase) can agree with this newly formed network structure with rational intermolecular hydrogen bonds. As revealed by the theoretical study,⁵³ bulk water strongly favors some rare G tautomers, and the most stable one (G/(3H,7H)), as shown in Fig. 10c is even energetically more favorable than the canonical G/9H form in the water environment. As further revealed by extensive density functional theory calculations, the key to facilitating the formation of this rare tautomer is proposed to be the “water bridge” which largely reduces the energy barriers of intramolecular proton-transfer processes. The DFT optimized model of the parallel six-membered ring network composed of G/(3H,7H) molecules is superimposed on the STM image shown in Fig. 10c. Also, a simulated STM image is partially overlaid on the close-up STM image as shown in Fig. 10b.

In the above mentioned case, water molecules are not directly involved in the network structure, and the regulation of the supramolecular nanostructure is achieved by water

induced tautomerization. By introducing water into another nucleobase system, Zhang *et al.*¹⁰⁴ investigated the dynamic hydration process of adenine (A) networks on Au(111) in real space, which resulted in controllable scission and stitching of adenine structures. It is known that A molecules can form both heterochiral and homochiral network structures on Au(111)^{68,69} (Fig. 11a and d, and the corresponding DFT-optimized structural models are shown in Fig. 11b and e). The exposure of the A-precured sample (held at RT) to the water atmosphere at a pressure of $\sim 10^{-6}$ mbar firstly leads to the disassembly of the A islands and simultaneous formation of molecular rows, which displays the scission of A networks induced by water molecules. Further exposure to the water atmosphere at a higher pressure of 3×10^{-5} mbar for 10 minutes results in structural transformation from molecular rows to two kinds of network structures with heterochiral or homochiral A molecules involved (Fig. 11c and f, and the corresponding DFT-optimized structural models and STM simulations superimposed on the close-up STM images are shown in Fig. 11h and i), in which the bright protrusions (highlighted by white circles) in between the A molecular rows are assigned to water molecules. Such network structures tend to grow larger with more and more water involved as shown in Fig. 11g, which indicates that the A molecular rows are further stitched by water molecules *via* hydrogen bonds. The whole process implies that water molecules may perturb the initial 2D self-assembled A islands (by selectively breaking the relatively weak hydrogen bonds)

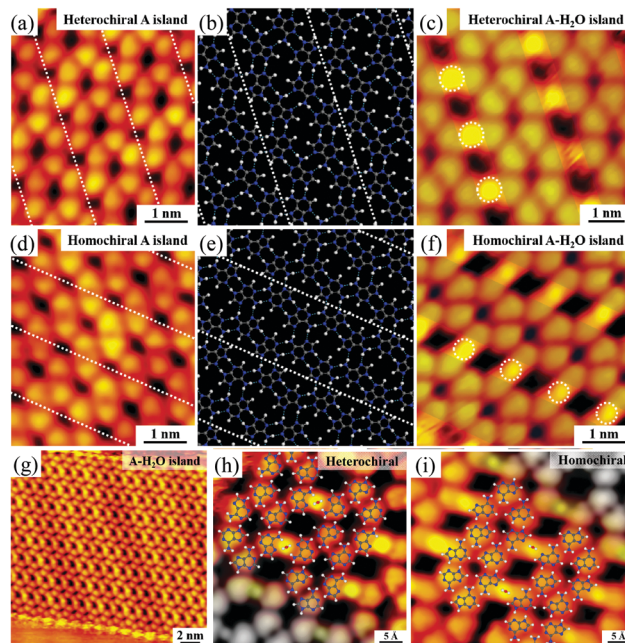


Fig. 11 (a and d) STM images of heterochiral and homochiral self-assembled A islands on Au(111). (b and e) The corresponding structural models of A islands. (c and f) STM images of the corresponding heterochiral and homochiral A-H₂O islands. (g) A large-scale STM image showing the formation of the A-H₂O island. (h and i) Close-up STM images partially superimposed with the corresponding DFT-optimized structural models and the STM simulations (the gray parts).¹⁰⁴ Reproduced with permission from Royal Society of Chemistry.

and induce them to dissociate into 1D molecular rows in the first step (*i.e.*, scission), and then reform the 2D A-H₂O networks *via* newly formed hydrogen bonds between water and A molecules (*i.e.*, stitching).

2D nanostructures constructed by nucleobases pairing

The adsorption and self-assembly of individual nucleobases on surfaces have been well studied by the surface science community in the past few decades.^{36,67–72} Later on, two different nucleobases have also been simultaneously introduced onto surfaces in which the specific molecular recognition based on the principle of complementary base-pairing has been investigated. Mamdouh *et al.*¹⁰⁵ showed the well-ordered supramolecular nanopatterns formed by mixing two complementary DNA bases (adenine and thymine) at the liquid (1-octanol solvent)/solid (graphite) interface for the first time. Similarly, coadsorption of guanine and uracil at the liquid/solid interface led to another kind of 2D supramolecular nanopatterns based on guanine–uracil wobble base pairs.¹⁰⁶ Later, Otero *et al.*¹⁰⁷ investigated the feasibility of molecular recognition in the complementary guanine and cytosine system under extremely clean UHV conditions on Au(111), which gave the first real-space evidence of guanine–cytosine Watson–Crick base pairs on the surfaces. On this basis, Xu *et al.*¹⁰⁸ codeposited the *N*-aryl-modified guanine and cytosine nucleobase derivatives onto the Au(111) surface under UHV conditions, and a highly ordered

supramolecular porous network based on Watson–Crick GC pairs was formed, which implied that molecular recognition was more efficient between base derivatives than archetypal nucleobases on surfaces.

More recently, Ding *et al.*¹⁰⁹ chose another pair of modified bases, *i.e.*, 9-methyladenine (9mA) and 1-ethyluracil (1eU), and achieved two different 2D self-assembled structures based on Watson–Crick (W–C) and Hoogsteen (H) AU base pairs on Au(111). Codeposition of the 1eU and 9mA molecules at a ratio of 1 : 1 and then annealing the sample at 330 K results in the coexistence of the two ordered phases (as shown in Fig. 12). From the STM images with submolecular resolution, we identify that the strip-like structure (Fig. 12a and b) is composed of the mixed W–C and H AU pairs, and the well-ordered 2D nanostructure (Fig. 12c and d) is composed of the pure H AU pairs.

Conclusions

In this article, we have summarized the strategies for designing and fabricating 2D well-defined molecular assemblies on the basis of nucleobases and various reactants (metals, halogens, salts, water) on Au(111), which demonstrate the potential and flexibility toward the formation of 2D biologically relevant molecular nanostructures on surfaces. These research studies show that various reactants have different effects when employed in the construction of 2D nanostructures. In general, metals interact with N and/or O binding sites of nucleobases resulting in various motifs *via* coordination or electrostatic interactions; halogens can induce structural transformation and stabilization of metal–organic motifs *via* hydrogen bonding; salts can simultaneously provide both metals and halogens; water may induce rare tautomerization or controllable breakage of some weak hydrogen bonds of the self-assembled structure. These findings provide a variety of approaches for the construction and regulation of nanostructures, which may shed light on the fabrication of DNA-based artificial molecular constructions on surfaces.¹³ Among others, the diverse metal–organic networks are one of the most ordered and stable 2D nanostructures, which have the potential application in nano-devices and biosensors. In addition, these experiments also increase fundamental understanding of interactions between nucleobases and other reactants, which may further provide theoretical basis and biological guidance for designing of anti-cancer drugs. Although various 2D nanostructures based on nucleobases have been achieved on surfaces, the research in this field still carries significant limitations. From a general perspective, there are few predicting properties and functionalities of these 2D biomolecular nanostructures, which make them far from practical applications. On the other hand, such an on-surface system especially under UHV conditions is still too simple in comparison with the real situations *in vivo*. With the aim of creating more and more sophisticated and complex nanostructures, especially with specific functionalities and potential applications, other molecular precursors like larger

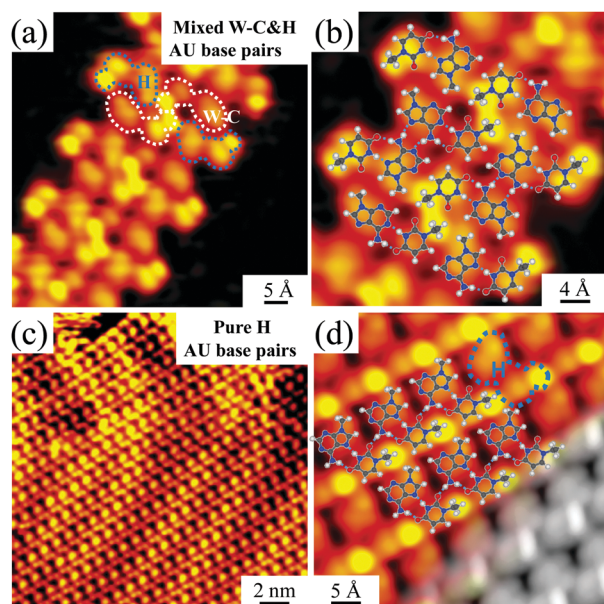


Fig. 12 STM images and DFT optimized models of self-assembled structures composed of different AU base pairs on Au(111). (a and b) STM images showing the structure composed of both Watson–Crick and Hoogsteen AU pairs. (c and d) STM images showing the structure composed of pure Hoogsteen AU pairs. The corresponding DFT-optimized models and the STM simulation (the gray part) are partially superimposed on the close-up STM images. Watson–Crick and Hoogsteen AU pairs are depicted by white and blue contours, also indicated by W–C and H notations, respectively.¹⁰⁹ Reproduced with permission from Royal Society of Chemistry.

biomolecules (e.g., nucleotides) should be considered to be involved in the model systems. Besides, considering the rapidly developing field of on-surface synthesis, it would be highly intriguing to employ nucleobases as molecular precursors to make covalently bonded surface nanostructures like artificial DNA structures to explore DNA sequencing and biosensors at the single-molecule level.

Conflicts of interest

There are no conflicts to declare.

Acknowledgements

The authors acknowledge financial support from the National Natural Science Foundation of China (21473123, 21622307, 21790351).

References

- J.-M. Lehn, *Angew. Chem., Int. Ed.*, 1988, **27**, 89.
- J. V. Barth, G. Costantini and K. Kern, *Nature*, 2005, **437**, 671.
- D. Bléger, D. Kreher, F. Mathevet, A.-J. Attias, G. Schull, A. Huard, L. Douillard, C. Fiorini-Debuischert and F. Charra, *Angew. Chem., Int. Ed.*, 2007, **119**, 7548.
- S. Furukawa, K. Tahara, F. C. De Schryver, M. Van der Auweraer, Y. Tobe and S. De Feyter, *Angew. Chem., Int. Ed.*, 2007, **119**, 2889.
- A. Kühnle, *Curr. Opin. Colloid Interface Sci.*, 2009, **14**, 157.
- C. A. Palma, J. Bjork, M. Bonini, M. S. Dyer, A. Llanes-Pallas, D. Bonifazi, M. Persson and P. Samori, *J. Am. Chem. Soc.*, 2009, **131**, 13062.
- T. Kudernac, S. Lei, J. A. A. W. Elemans and S. De Feyter, *Chem. Soc. Rev.*, 2009, **38**, 402.
- Y. Yang and C. Wang, *Chem. Soc. Rev.*, 2009, **38**, 2576.
- Y. Yang and C. Wang, *Curr. Opin. Colloid Interface Sci.*, 2009, **14**, 135.
- R. Gutzler, T. Sirtl, J. F. Dienstmaier, K. Mahata, W. M. Heckl, M. Schmittl and M. Lackinger, *J. Am. Chem. Soc.*, 2010, **132**, 5084.
- M. O. Blunt, J. Adisoejoso, K. Tahara, K. Katayama, M. Van der Auweraer, Y. Tobe and S. De Feyter, *J. Am. Chem. Soc.*, 2013, **135**, 12068.
- Y. Liu, L. Mu, B. Liu and J. Kong, *Chem. – Eur. J.*, 2005, **11**, 2622.
- J. L. Sessler and J. Jayawickramarajah, *Chem. Commun.*, 2005, 1939.
- T. Kudernac, N. Ruangsupapichat, M. Parschau, B. Macia, N. Katsonis, S. R. Harutyunyan, K.-H. Ernst and B. L. Feringa, *Nature*, 2011, **479**, 208.
- B. E. Hirsch, K. P. McDonald, B. Qiao, A. H. Flood and S. L. Tait, *ACS Nano*, 2014, **8**, 10858.
- F. P. Cometto, K. Kern and M. Lingenfelder, *ACS Nano*, 2015, **9**, 5544.
- S.-L. Lee, Y. Fang, G. Velpula, F. P. Cometto, M. Lingenfelder, K. Müllen, K. S. Mali and S. De Feyter, *ACS Nano*, 2015, **9**, 11608.
- A. Dmitriev, H. Spillmann, N. Lin, J. V. Barth and K. Kern, *Angew. Chem., Int. Ed.*, 2003, **115**, 2774.
- T. Classen, G. Fratesi, G. Costantini, S. Fabris, F. L. Stadler, C. Kim, S. de Gironcoli, S. Baroni and K. Kern, *Angew. Chem., Int. Ed.*, 2005, **117**, 6298.
- J. V. Barth, *Annu. Rev. Phys. Chem.*, 2007, **58**, 375.
- J. V. Barth, *Surf. Sci.*, 2009, **603**, 1533.
- K. S. Mali, D. Wu, X. Feng, K. Müllen, M. Van der Auweraer and S. De Feyter, *J. Am. Chem. Soc.*, 2011, **133**, 5686.
- L. Dong, Q. Sun, C. Zhang, Z. Li, K. Sheng, H. Kong, Q. Tan, Y. Pan, A. Hu and W. Xu, *Chem. Commun.*, 2013, **49**, 1735.
- W. Xu, C. Zhang, H. Gersen, Q. Sun, H. Kong, L. Dong, K. Sheng, Q. Tan, E. Lægsgaard and F. Besenbacher, *Chem. Commun.*, 2013, **49**, 5207.
- Q. Sun, C. Zhang, L. Cai, Q. Tan and W. Xu, *Chem. Commun.*, 2014, **50**, 12112.
- Q. Tan, C. Zhang, N. Wang, X. Zhu, Q. Sun, M. F. Jacobsen, K. V. Gothelf, F. Besenbacher, A. Hu and W. Xu, *Chem. Commun.*, 2014, **50**, 356.
- C. Zhang, Q. Sun, K. Sheng, Q. Tan and W. Xu, *Nanoscale*, 2014, **6**, 11062.
- J. Shang, Y. Wang, M. Chen, J. Dai, X. Zhou, J. Kuttner, G. Hilt, X. Shao, J. M. Gottfried and K. Wu, *Nat. Chem.*, 2015, **7**, 389.
- Q. Sun, L. Cai, H. Ma, C. Yuan and W. Xu, *Chem. Commun.*, 2015, **51**, 14164.
- G. Lyu, Q. Zhang, J. I. Urgel, G. Kuang, W. Auwärter, D. Ecija, J. V. Barth and N. Lin, *Chem. Commun.*, 2016, **52**, 1618.
- J. I. Urgel, D. Ecija, G. Lyu, R. Zhang, C.-A. Palma, W. Auwärter, N. Lin and J. V. Barth, *Nat. Chem.*, 2016, **8**, 657.
- M. Bao, X. Wei, L. Cai, Q. Sun, Z. Liu and W. Xu, *Phys. Chem. Chem. Phys.*, 2017, **19**, 18704.
- L. Cai, Q. Sun, M. Bao, H. Ma, C. Yuan and W. Xu, *ACS Nano*, 2017, **11**, 3727.
- Y. Zhang, Y. Ding, L. Xie, H. Ma, X. Yao, C. Zhang, C. Yuan and W. Xu, *ChemPhysChem*, 2017, **18**, 3544.
- Q. Fan, L. Liu, J. Dai, T. Wang, H. Ju, J. Zhao, J. Kuttner, G. Hilt, J. M. Gottfried and J. Zhu, *ACS Nano*, 2018, **12**, 2267.
- A. C. Papageorgiou, S. Fischer, J. Reichert, K. Diller, F. Blobner, F. Klappenberger, F. Allegretti, A. P. Seitsonen and J. V. Barth, *ACS Nano*, 2012, **6**, 2477.
- H. Yan, L. Feng, T. H. LaBean and J. H. Reif, *J. Am. Chem. Soc.*, 2003, **125**, 14246.
- N. C. Seeman, *Nature*, 2003, **421**, 427.
- H. Yan, S. H. Park, G. Finkelstein, J. H. Reif and T. H. LaBean, *Science*, 2003, **301**, 1882.
- D. Liu, S. H. Park, J. H. Reif and T. H. LaBean, *PNAS*, 2004, **101**, 717.
- K. V. Gothelf and T. H. LaBean, *Org. Biomol. Chem.*, 2005, **3**, 4023.
- P. M. Mendes, *Chem. Soc. Rev.*, 2008, **37**, 2512.
- K. Szczepaniak, M. Szczesniak, W. Szajda, W. B. Person and J. Leszczynski, *Can. J. Chem.*, 1991, **69**, 1705.
- C. Colominas, F. J. Luque and M. Orozco, *J. Am. Chem. Soc.*, 1996, **118**, 6811.
- L. Gorb and J. Leszczynski, *J. Am. Chem. Soc.*, 1998, **120**, 5024.
- J. Gu and J. Leszczynski, *J. Phys. Chem. A*, 1999, **103**, 2744.
- J. Šponer, J. E. Šponer, L. Gorb, J. Leszczynski and B. Lippert, *J. Phys. Chem. A*, 1999, **103**, 11406.
- E. S. Kryachko, M. T. Nguyen and T. Zeegers-Huyskens, *J. Phys. Chem. A*, 2001, **105**, 1934.
- G. Fogarasi and P. G. Szalay, *Chem. Phys. Lett.*, 2002, **356**, 383.
- M. Mons, I. Dimicoli, F. Piuze, B. Tardivel and M. Elhanine, *J. Phys. Chem. A*, 2002, **106**, 5088.
- M. K. Shukla and J. Leszczynski, *J. Phys. Chem. A*, 2002, **106**, 11338.
- S. A. Trygubenko, T. V. Bogdan, M. Rueda, M. Orozco, F. J. Luque, J. Šponer, P. Slaviček and P. Hobza, *Phys. Chem. Chem. Phys.*, 2002, **4**, 4192.
- M. Hanus, F. Ryjáček, M. Kabeláč, T. Kubař, T. V. Bogdan, S. A. Trygubenko and P. Hobza, *J. Am. Chem. Soc.*, 2003, **125**, 7678.
- M. Hanus, M. Kabeláč, J. Rejnek, F. Ryjáček and P. Hobza, *J. Phys. Chem. B*, 2004, **108**, 2087.
- A. Abo-Riziq, B. Crews, L. Grace and M. S. de Vries, *J. Am. Chem. Soc.*, 2005, **127**, 2374.
- K. C. Hunter, L. R. Rutledge and S. D. Wetmore, *J. Phys. Chem. A*, 2005, **109**, 9554.
- J. Rejnek, M. Hanus, M. Kabeláč, F. Ryjáček and P. Hobza, *Phys. Chem. Chem. Phys.*, 2005, **7**, 2006.
- M. Kabeláč and P. Hobza, *J. Phys. Chem. B*, 2006, **110**, 14515.
- A. Abo-riziq, B. O. Crews, I. Compagnon, J. Oomens, G. Meijer, G. Von Helden, M. Kabeláč, P. Hobza and M. S. de Vries, *J. Phys. Chem. A*, 2007, **111**, 7529.
- M. Kabeláč and P. Hobza, *Phys. Chem. Chem. Phys.*, 2007, **9**, 903.
- J. Rejnek and P. Hobza, *J. Phys. Chem. B*, 2007, **111**, 641.
- T. Zelený, P. Hobza and M. Kabeláč, *Phys. Chem. Chem. Phys.*, 2009, **11**, 3430.
- H. T. Zheng, D. X. Zhao and Z. Z. Yang, *Chin. J. Chem.*, 2011, **29**, 2243.
- C. Bistafa, H. C. Georg and S. Canuto, *Comput. Theor. Chem.*, 2014, **1040-1041**, 312.
- S. Ø. Pedersen, C. S. Byskov, F. Turecek and S. B. Nielsen, *J. Phys. Chem. A*, 2014, **118**, 4256.

- 66 H. Kong, L. Wang, Q. Sun, C. Zhang, Q. Tan and W. Xu, *Angew. Chem., Int. Ed.*, 2015, **54**, 6526.
- 67 T. Dretschkow, A. S. Dakkouri and T. Wandlowski, *Langmuir*, 1997, **13**, 2843.
- 68 R. E. A. Kelly, W. Xu, M. Lukas, R. Otero, M. Mura, Y.-J. Lee, E. Lægsgaard, I. Stensgaard, L. N. Kantorovich and F. Besenbacher, *Small*, 2008, **4**, 1494.
- 69 M. Lukas, R. E. A. Kelly, L. N. Kantorovich, R. Otero, W. Xu, E. Lægsgaard, I. Stensgaard and F. Besenbacher, *J. Chem. Phys.*, 2009, **130**, 024705.
- 70 R. Otero, M. Lukas, R. E. A. Kelly, W. Xu, E. Lægsgaard, I. Stensgaard, L. N. Kantorovich and F. Besenbacher, *Science*, 2008, **319**, 312.
- 71 W. Xu, R. E. A. Kelly, H. Gersen, E. Lægsgaard, I. Stensgaard, L. N. Kantorovich and F. Besenbacher, *Small*, 2009, **5**, 1952.
- 72 W. Xu, R. E. A. Kelly, R. Otero, M. Schöck, E. Lægsgaard, I. Stensgaard, L. N. Kantorovich and F. Besenbacher, *Small*, 2007, **3**, 2011.
- 73 A. M. Zahler, J. R. Williamson, T. R. Cech and D. M. Prescott, *Nature*, 1991, **350**, 718.
- 74 W. Xu, Q. Tan, M. Yu, Q. Sun, H. Kong, E. Lægsgaard, I. Stensgaard, J. Kjems, J. G. Wang, C. Wang and F. Besenbacher, *Chem. Commun.*, 2013, **49**, 7210.
- 75 W. Xu, J. G. Wang, M. Yu, E. Lægsgaard, I. Stensgaard, T. R. Linderoth, B. Hammer, C. Wang and F. Besenbacher, *J. Am. Chem. Soc.*, 2010, **132**, 15927.
- 76 H. Kong, Q. Sun, L. Wang, Q. Tan, C. Zhang, K. Sheng and W. Xu, *ACS Nano*, 2014, **8**, 1804.
- 77 H. Kong, C. Zhang, L. Xie, L. Wang and W. Xu, *Angew. Chem., Int. Ed.*, 2016, **55**, 7157.
- 78 L. Wang, H. Kong, C. Zhang, Q. Sun, L. Cai, Q. Tan, F. Besenbacher and W. Xu, *ACS Nano*, 2014, **8**, 11799.
- 79 C. Zhang, L. Wang, L. Xie, Y. Ding and W. Xu, *Chem. – Eur. J.*, 2017, **23**, 2356.
- 80 C. Zhang, L. Xie, Y. Ding, C. Yuan and W. Xu, *Phys. Chem. Chem. Phys.*, 2018, **20**, 3694.
- 81 L. Xie, C. Zhang, Y. Ding and W. Xu, *Angew. Chem., Int. Ed.*, 2017, **56**, 5077.
- 82 C. K. Chiang, C. R. Fincher, Y. W. Park, A. J. Heeger, H. Shirakawa, E. J. Louis, S. C. Gau and A. G. MacDiarmid, *Phys. Rev. Lett.*, 1977, **39**, 1098.
- 83 D. Kumar and R. C. Sharma, *Eur. Polym. J.*, 1998, **34**, 1053.
- 84 C. Zhang, Q. Sun, H. Chen, Q. Tan and W. Xu, *Chem. Commun.*, 2015, **51**, 495.
- 85 Q. Fan, J. M. Gottfried and J. Zhu, *Acc. Chem. Res.*, 2015, **48**, 2484.
- 86 Q. Sun, L. Cai, H. Ma, C. Yuan and W. Xu, *ACS Nano*, 2016, **10**, 7023.
- 87 Q. Sun, L. Cai, H. Ma, C. Yuan and W. Xu, *Chem. Commun.*, 2016, **52**, 6009.
- 88 M. Bieri, M.-T. Nguyen, O. Gröning, J. Cai, M. Treier, K. Ait-Mansour, P. Ruffieux, C. A. Pignedoli, D. Passerone, M. Kastler, K. Müllen and R. Fasel, *J. Am. Chem. Soc.*, 2010, **132**, 16669.
- 89 L. Lafferentz, V. Eberhardt, C. Dri, C. Africh, G. Comelli, F. Esch, S. Hecht and L. Grill, *Nat. Chem.*, 2012, **4**, 215.
- 90 T. Kaposi, S. Joshi, T. Hoh, A. Wiengarten, K. Seufert, M. Paszkiewicz, F. Klappenberger, D. Eciija, L. Dordevic, T. Marangoni, D. Bonifazi, J. V. Barth and W. Auwärter, *ACS Nano*, 2016, **10**, 7665.
- 91 A. Rastgoo-Lahrood, J. Björk, M. Lischka, J. Eichhorn, S. Kloft, M. Fritton, T. Strunskus, D. Samanta, M. Schmittel, W. M. Heckl and M. Lackinger, *Angew. Chem., Int. Ed.*, 2016, **128**, 7780.
- 92 C. Wäckerlin, C. Iacovita, D. Chylarecka, P. Fesser, T. A. Jung and N. Ballav, *Chem. Commun.*, 2011, **47**, 9146.
- 93 D. Skomski, S. Abb and S. L. Tait, *J. Am. Chem. Soc.*, 2012, **134**, 14165.
- 94 D. Skomski and S. L. Tait, *J. Phys. Chem. C*, 2013, **117**, 2959.
- 95 T. K. Shimizu, J. Jung, H. Imada and Y. Kim, *Angew. Chem., Int. Ed.*, 2014, **126**, 13949.
- 96 C. Zhang, L. Wang, L. Xie, H. Kong, Q. Tan, L. Cai, Q. Sun and W. Xu, *ChemPhysChem*, 2015, **16**, 2099.
- 97 C. Zhang, L. Xie, L. Wang, H. Kong, Q. Tan and W. Xu, *J. Am. Chem. Soc.*, 2015, **137**, 11795.
- 98 H. Kong, L. Wang, Q. Tan, C. Zhang, Q. Sun and W. Xu, *Chem. Commun.*, 2014, **50**, 3242.
- 99 L. Xie, C. Zhang, Y. Ding, W. E. C. Yuan and W. Xu, *Chem. Commun.*, 2017, **53**, 8767.
- 100 Y. Ding, L. Xie, C. Zhang and W. Xu, *Chem. Commun.*, 2017, **53**, 9846.
- 101 J. Henzl, K. Boom and K. Morgenstern, *J. Am. Chem. Soc.*, 2014, **136**, 13341.
- 102 J. Henzl, K. Boom and K. Morgenstern, *J. Chem. Phys.*, 2015, **142**, 101920.
- 103 C. Zhang, L. Xie, Y. Ding, Q. Sun and W. Xu, *ACS Nano*, 2016, **10**, 3776.
- 104 C. Zhang, L. Xie, Y. Ding and W. Xu, *Chem. Commun.*, 2018, **54**, 771.
- 105 W. Mamdouh, M. Dong, S. Xu, E. Rauls and F. Besenbacher, *J. Am. Chem. Soc.*, 2006, **128**, 13305.
- 106 W. Mamdouh, R. E. A. Kelly, M. Dong, L. N. Kantorovich and F. Besenbacher, *J. Am. Chem. Soc.*, 2008, **130**, 695.
- 107 R. Otero, W. Xu, M. Lukas, R. E. A. Kelly, E. Lægsgaard, I. Stensgaard, J. Kjems, L. N. Kantorovich and F. Besenbacher, *Angew. Chem., Int. Ed.*, 2008, **47**, 9673.
- 108 W. Xu, J. G. Wang, M. F. Jacobsen, M. Mura, M. Yu, R. E. A. Kelly, Q. Q. Meng, E. Lægsgaard, I. Stensgaard, T. R. Linderoth, J. Kjems, L. N. Kantorovich, K. V. Gothelf and F. Besenbacher, *Angew. Chem., Int. Ed.*, 2010, **49**, 9373.
- 109 Y. Ding, L. Xie, X. Yao and W. Xu, *Chem. Commun.*, 2018, **54**, 3715.